

SUPPORTING INFORMATION

Tailoring the facet distribution on copper with chloride

Pedro Mazaira Couce^a, Thor Kongstad Madsen^a, Elena Plaza-Mayoral^a, Henrik H.

Kristoffersen^{*,a}, Ib Chorkendorff^b, Kim Nicole Dalby^c, Ward van der Stam^d, Jan Rossmeisl^a,

María Escudero-Escribano^{*a,e,f}, Paula Sebastián-Pascual^{*,a}.

- a. Department of Chemistry, Center of High Entropy Catalysis (CHEAC) University of Copenhagen, Universitetsparken 5, 2100 Copenhagen, Denmark
- b. Department of Physics, Surface Physics and Catalysis, Technical University of Denmark, Fysikvej, DK-2800 Lyngby, Denmark
- c. Topsoe A/S, Haldor Topsøes Allé 1, DK-2800 Kgs. Lyngby, Denmark
- d. Utrecht University, Inorganic Chemistry and Catalysis, Debye Institute for Nanomaterials Science, Netherlands
- e. Catalan Institute of Nanoscience and Nanotechnology (ICN2), CSIC, Barcelona Institute of Science and Technology, UAB Campus, 08193 Bellaterra, Barcelona, Spain
- f. ICREA, Pg. Lluís Companys 23, 08010 Barcelona, Spain

*Corresponding authors:

Paula Sebastián-Pascual: paula.pascual@chem.ku.dk

María Escudero-Escribano: maria.escudero@icn2.cat

Henrik H Kristoffersen: hkh@chem.ku.dk

1. Electrode preparation and stability of the lead UPD voltammetric fingerprint.

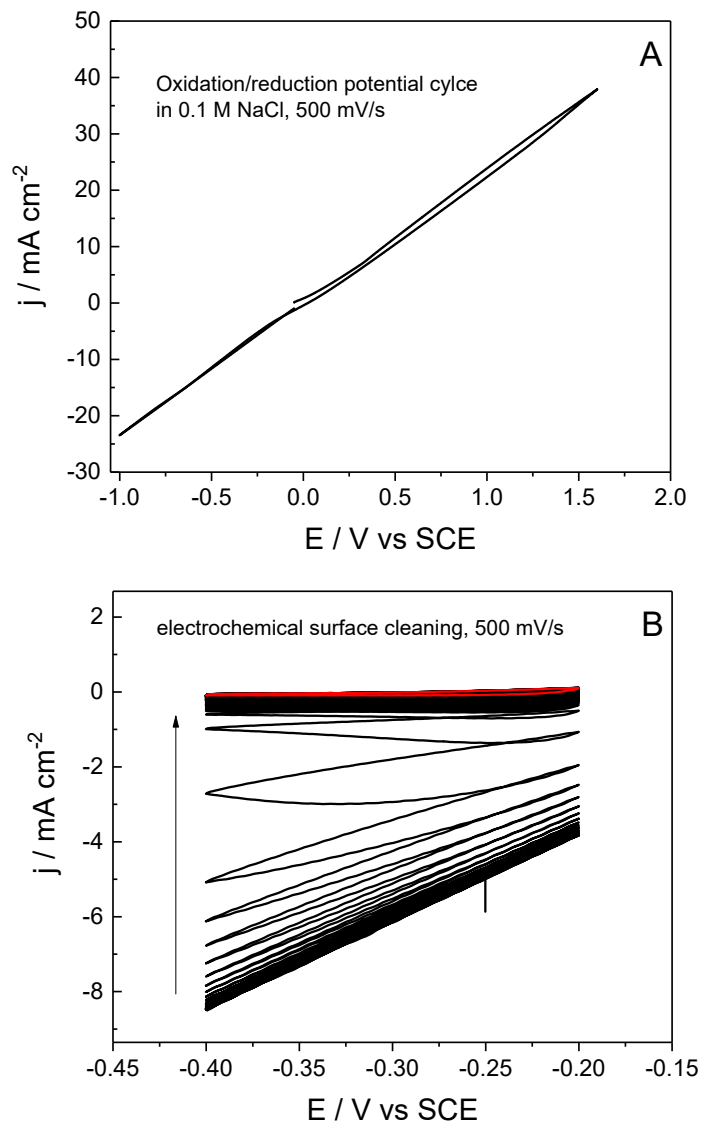


Figure S1: A) Voltammetric oxidation reduction treatment of the Cu(poly) in the 0.1 M NaCl solution, at 500 mV/s, to induce surface refaceting. B) Electrochemical surface cleaning and removal of the copper chloride layer in the 0.1 M NaCl solution. In this electrochemical surface cleaning we apply consecutive cycles at 500 mV/s until we obtain a constant capacitive current (red line).

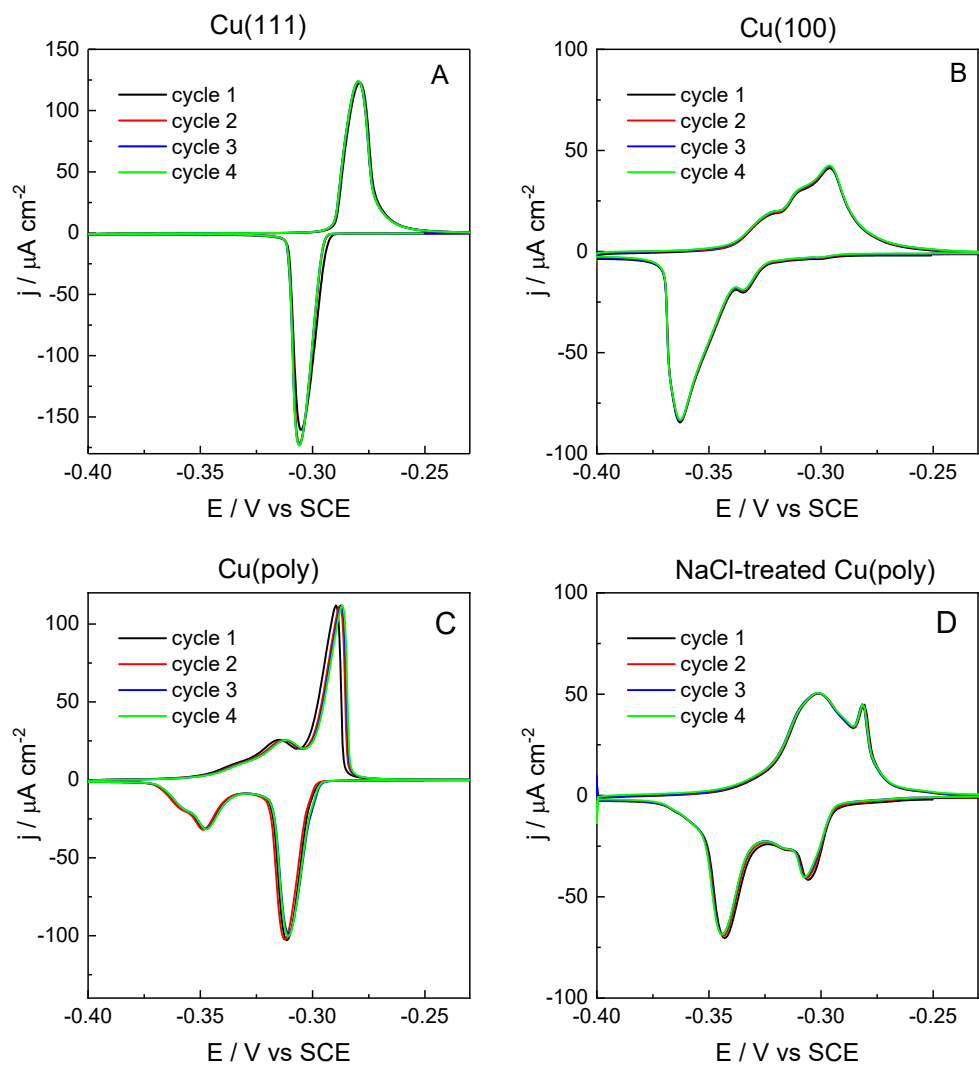


Figure S2: Consecutive voltammetric cycles of the lead UPD at 5 mV/s and in a 0.1 M KClO_4 + 2mM PbClO_4 +2 mM NaCl solution at pH 2.9, recorded on A) Cu(111), B) Cu(100), C) Cu(poly) and D) NaCl-treated Cu(poly) with an upper applied potential of 1.6 V vs SCE.

2. Peak-potential and electroactive surface area of the different Cu(hkl) and multifaceted copper.

Table S1: Cathodic peak potential values of the lead UPD recorded on Cu single crystalline electrodes at 5 mV/s and in a 0.1 M KClO₄ + 2mM PbClO₄ solution at pH 2.9.

Peak potential values on Cu single crystalline electrodes				
	Cu(111)	Cu(110)	Cu(310)	Cu(100)
	Peak 1	Peak 1 Peak 2	Peak 1	Peak 1 Peak 2
Peak potential / V vs SCE	-0.305 ± 0.002	-0.276 ± 0.001 -0.318 ± 0.002	-0.340 ± 0.001	-0.333 ± 0.001 -0.362 ± 0.002

Table S2: Integrated charge values of the cathodic voltammetric region of the lead UPD on different Cu surfaces.

Electrode	Cu(111)	Cu(100)	Cu(110)	Cu(310)
Integrated charge / μC cm⁻²	350 ± 10	375 ± 19	338 ± 11	316.0±0.4
Electrode	Cu roughened in 0.1 M NaCl			
Upper potential limit / V vs SCE	Cu(poly)	1.30 V	1.6 V	2.0 V
Integrated charge / μC cm⁻²	367±25	382 ± 56	378 ± 63	435 ± 70
Roughness factor*	1	1.05 ± 0.03	1.04 ± 0.05	1.19 ± 0.07

*The roughness factors have been calculated by dividing the integrated charge of the Cu(poly) surface treated in NaCl solution by the Cu(poly) charge measured prior to the treatment in NaCl.

3. Peak deconvolution and facet-distribution on Cu.

To perform the peak deconvolution and simulation of the curves, we have used mathematical gaussian functions using origin software. Relative good fitting of the peaks is obtained and the simulated and experimental curves almost overlap. We note that sometimes the overlapping is not wholly perfect (Fig. S3), a fact that we ascribe to irregularities and imperfections on the surfaces after being electrochemically treated in 0.1 M NaCl.

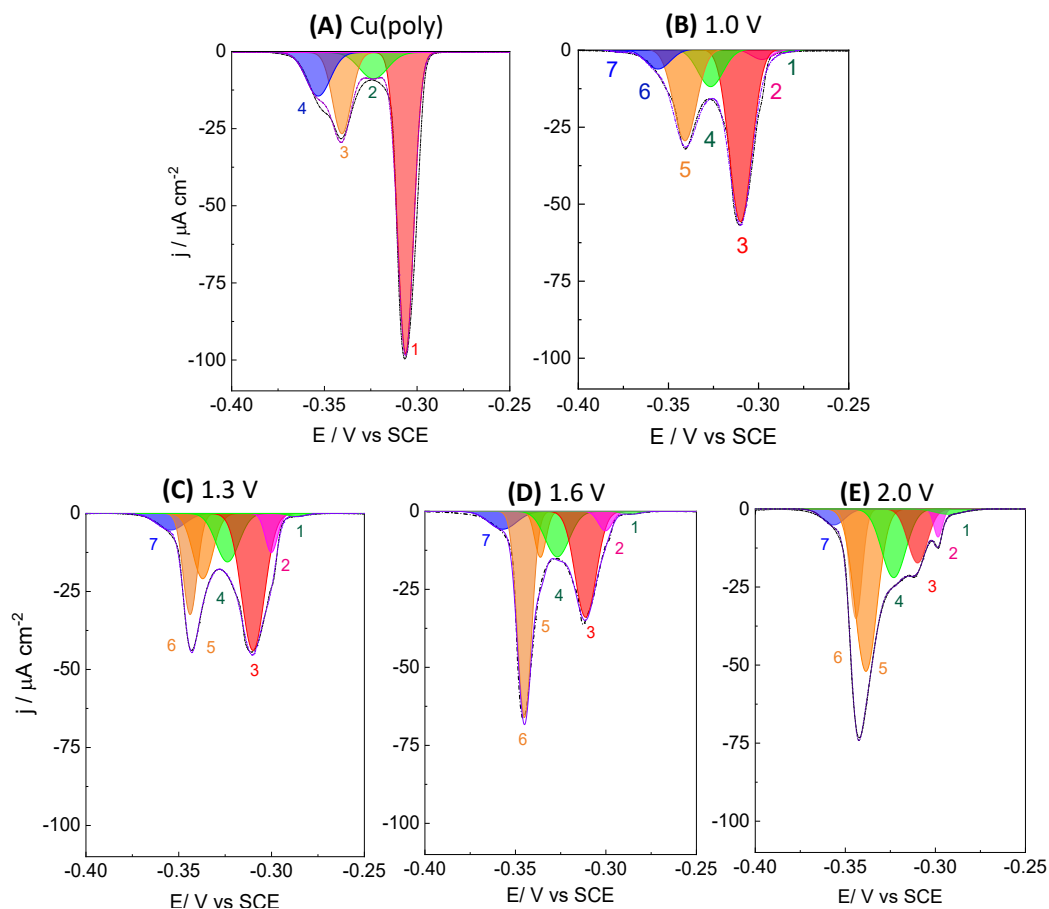


Figure S3: Peak deconvolution of the cathodic region of the the lead UPD CVs at 5 mV/s and in a 0.1 M $\text{KClO}_4 + 2\text{mM PbClO}_4$ solution at pH 2.9, recorded on: **(A)** An electropolished Cu polycrystalline surfaces. A Cu polycrystalline surface that was restructured in a 0.1M NaCl solution by applying a negative voltage of -1.0 V vs SCE and an oxidation potential limit of: **(B)** 1.0 V vs SCE, **(C)** 1.3 V vs SCE, **(D)** 1.6 V vs SCE and **(E)** 2.0 V vs SCE. We also indicate the number of peaks in each deconvolution. Based on the lead UPD CVs on Cu single crystalline electrodes in Figure 1A, we suggest that, approximately, red peaks corresponds to $\langle 111 \rangle$ domains, orange peaks corresponds to $\langle 310 \rangle$ domains and blue peaks are $\langle 100 \rangle$ or $n(100) \times (110)$ domains

with larger (100) terraces. Purple and green peaks are more difficult to attribute and may contain contributions of (110) domains and step sites.

Table S3: Peak analysis of the cathodic region of the lead UPD voltammetric curved from Figure SX. We provide the peak potential / V, the fraction of the integrated area and the width at the half maximum (mV) of each peak is provided. The deconvolution of the peaks in the CVs in Figure SX has been performed by applying a Gaussian function and using OriginPro 2020 software.

(A) Electro polished Cu					region	area
	Peak 1	Peak 2	Peak 3	Peak 4		
Peak potential / V vs SCE	-0.306	-0.323	-0.340	-0.353	<111>	0.59
fraction area	0.59	0.09	0.19	0.13	<310>	0.19
width (mV)	8.9	15.0	10.0	13.0		

(B) Cu roughened in 0.1 M NaCl at 1.0 V vs SCE								region	area
	Peak 1	Peak 2	Peak 3	Peak 4	Peak 5	Peak6	Peak7		
Peak potential / V vs SCE	-0.286	-0.298	-0.310	-0.327	-0.348	-0.356	-0.376	<111>	0.53
fraction area	0.01	0.03	0.50	0.12	0.27	0.06	0.01	<310>	0.27
width (mV)	14.6	14.0	14.6	16.2	14.9	16	14.6		

(C) Cu roughened in 0.1 M NaCl at 1.3 V vs SCE								region	area
	Peak 1	Peak 2	Peak 3	Peak 4	Peak 5	Peak6	Peak7		
Peak potential / V vs SCE	-0.286	-0.300	-0.310	-0.322	-0.337	-0.344	-0.354	<111>	0.45
fraction area	0.01	0.06	0.39	0.14	0.16	0.18	0.06	<310>	0.34
width (mV)	10.5	7.7	14.4	14.5	12.6	8.8	17.8		

(D) Cu roughened in 0.1 M NaCl at 1.6 V vs SCE								region	area
	Peak 1	Peak 2	Peak 3	Peak 4	Peak 5	Peak6	Peak7		
Peak potential / V vs SCE	-0.286	-0.300	-0.311	-0.327	-0.336	-0.345	-0.357	<111>	0.33
fraction area	0.01	0.04	0.29	0.15	0.07	0.38	0.07	<310>	0.45
width (mV)	12.0	9.0	13.6	15.6	7.3	9.1	18.0		

(E) Cu roughened in 0.1 M NaCl at 2.0 V vs SCE								region	area
	Peak 1	Peak 2	Peak 3	Peak 4	Peak 5	Peak6	Peak7		
Peak potential / V vs SCE	-0.292	-0.299	-0.310	-0.323	-0.339	-0.344	-0.356	<111>	0.13
fraction area	0.018	0.029	0.126	0.196	0.427	0.162	0.042	<310>	0.59

width (mV)	18.1	5.7	12.8	15.6	14.3	8.1	14.3
------------	------	-----	------	------	------	-----	------

4. Additional scanning electron microscopy images.

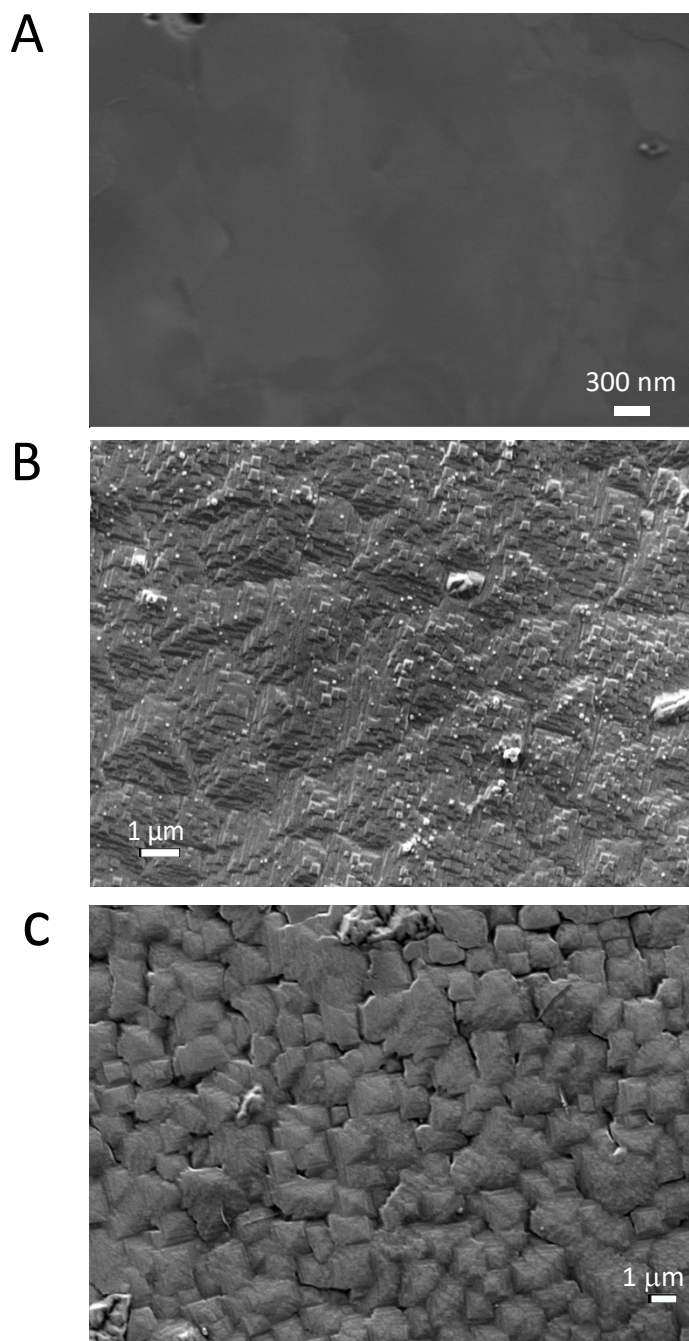


Figure S4: (A) Field emission scanning electron microscopy of an electropolished Cu polycrystalline electrode. Scanning electron microscopy images of: (B) Cu(poly) surface

restructured in a 0.1M NaCl solution at 1.6 V vs SCE. (C) Cu(poly) surface restructured in a 0.1 M NaCl solution at 2.0 V vs SCE.

5. X-ray photoelectron spectroscopy of a Cu treated in 0.1M NaOH solution.

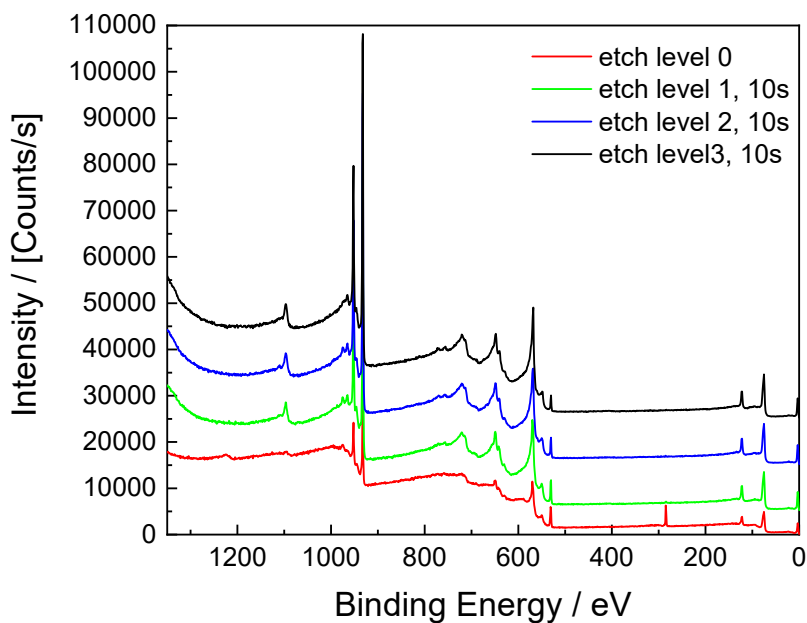


Figure S5: Survey of the XPS analysis of a Cu sample re-faceted in a 0.1 M NaCl solution at 2.0 V vs SCE. Then the sample was cycled in the double layer region until removing the passivation layer and obtaining a stable blank cyclic voltammetry in the same solution.

The survey was analysed before and after sputtering. We can note a Carbon 1s peak centred at 284.8 eV in the first scan (etch level 0). After only 10 seconds of sputtering, the C1s peak disappears. We attribute this carbon presence to the ambient and rest of the carbon-based samples that were analysed at the same time. Most importantly, the O1s peak decreases with sputtering. Regarding the Cu2p peak, it increases in intensity and becomes sharper after sputtering. The presence of Cl is not detected in the survey.

Figure S6: XPS analysis of Cu sample re-faceted in a 0.1 M NaCl solution by applying two potential cycles at 500 mV/s between -1.0 V and 2.0 V vs SCE. Then the sample was cycled in the double layer region until removing the passivation layer and obtaining a stable blank cyclic voltammery in the same solution. A) Cl 2p spectrum, each level 0: not surface etching, each level 3: 30 s surface etching. Cu 2p spectrum B) no surface etching, C) 30s of etching.

Fig. S6 A shows the XPS spectrum of chloride in our sample.¹² The chloride spectrum is characterized by a Cl2p peak at a binding energy of 189.5-199eV for metal chlorides. However, our XPS analysis does not detect any chloride component in this range. These results suggest that most of the formed copper chloride has been eliminated during the electrochemical sample preparation or it is below the detection limit of the technique. Figure S6 B and C show the Cu spectrum before and after sputtering which split in two spin-orbit components: Cu 2p_{1/2} and Cu2p_{3/2}. Cu 2p_{3/2} from Cu₂O and metallic Cu overlap at ca. 933eV. Additionally, a Cu 2p_{1/2} peak from Cu and Cu₂O appear at approximately 952.4 eV. We can identify the characteristic weak satellites from CuO at c.a. 945eV. The atomic percentage of oxygen in the sample before sputtering is ca. 47 %, which decreased to 16 %, after 30 s of sputtering in which a few surface nm were removed (Figure S4 C and S5). In contrast the atomic percentage of Cu has increased from 50 to 84%. This result suggests that Cu₂O remains at the surface while the core- is essentially metallic Cu, and therefore the features observed in the SEM arise from surface re-construction induced by chloride. We ascribe the formation of surface copper oxide to. 1) cleaning the samples with abundant milli-Q water before performing the ex-situ analysis. 2) Long exposure of the sample to air before the XPS analysis.

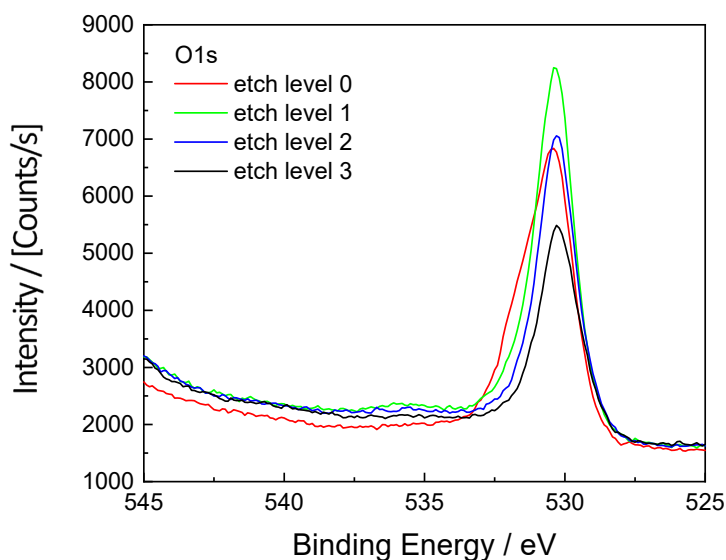


Figure S7: XPS analysis of the NaCl-treated Cu sample. O 1s spectrum with different sputtering levels.

The first O1s scan before sputtering (red line) is deconvoluted into two peaks. The peak centred at 530.3 corresponds to the metal oxides while the peak centred at 531.7 corresponding to organic C=O (usually found between 531.5–532 eV). This second peaks is related with the found C1s detected in the survey. After sputtering, the O1s peak becomes sharper and smaller each etch level. A single peak centred at 530eV is detected at level three of etching, which confirms that there is still some oxide species in our surface after sputtering.

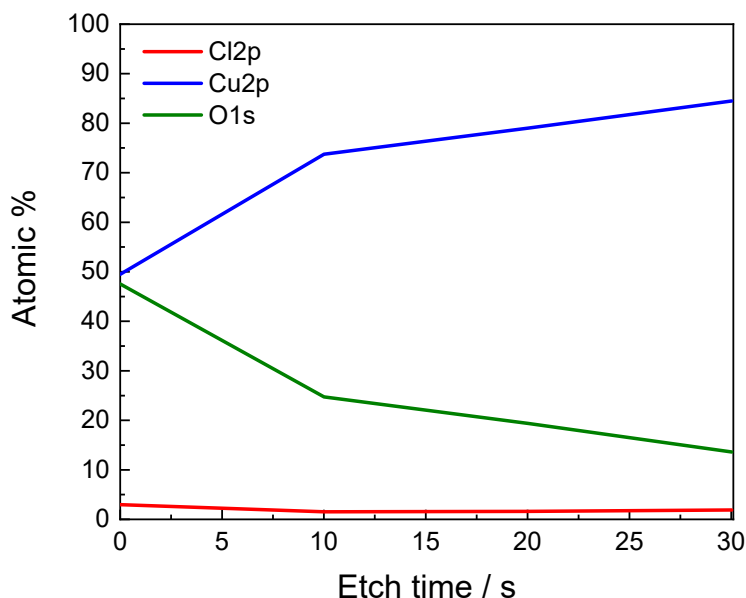


Figure S8: Plot of atomic percentage of relevant elements for this analysis, as a function of the etching time.

Figure S8 shows a profile of the atomic percentage of each element as a function of the sputtering time. Three levels of etching have been applied, each of them with 10 s of sputtering. The atomic percentage of oxygen highly decreases with time, whereas the atomic percentage of Cu rises, which suggest the presence of copper oxide only at the superficial layers of the deposits and on top of metallic copper.

6. Adsorption energies of chloride onto different single facets and Wulff constructions.

Computational Details

All calculations are calculated in GPAW version 22.1.0, with the BEEF-vdW functional native coded in GPAW. The density was described by plane-waves methodology with a 600 eV cut off. Structures were relaxed to less than 0.03 eV/Å. Boundary condition is applied in the style of a flat torus. K-points were sampled at 4×4×1 for the adsorbed calculations and 1×1×1 for the chlorine gas calculation.³

Harmonic approximation implemented in ASE⁴ was used for the vibrational calculation. This was calculated with a (310) surface with one chlorine atom on each side and was used to approximate all other surfaces. The copper atoms and the chlorine atom on the bottom surface were constraint to their relaxed position and only the chlorine atom on the top surface was moved.

File System

The calculation folders containing the data follow a naming pattern starting with denoting the facet, then the adsorbate, then the number of adsorbates on one side and lastly the number of surface atoms on one side. for example, 111-Cl-4per9 is the (111) facet with four chlorine adsorbates on a slab with 9 surface atoms. The surface atoms of the (111) facet is counted as the atoms in the raised rows. For the (310) facet the surface atoms are counted as 2 rows of each shelf. All files and scripts can be found at:⁵

Thermodynamic

The adsorption energy is defined as equation S1. Were E_{slab} is the calculated DFT energy for the system without chlorine on and E_{total} is the calculated DFT energy with chlorine.

$$G_{Cl^-} = \frac{E_{Cl_2}}{2} + (eU_{vs SHE} - 1.36V) + k_B T \ln 0.1 \quad (S1)$$

$$\Delta E_{adsorp}^{avg}(U) = \frac{E_{total} - E_{slab} - N_{Cl} G_{Cl^-}(U)}{N_{Cl}}$$

Table S4: a: Calculated, b: read from NIST².

	Cl*		Cl ₂ (g)
$Z_{p\ bound}$	0.03 eV (a)	$Z_{p\ gas}$	0.049 eV (a)
$-S_{bound} \cdot T$	-0.108 eV (a)	$-S_{gas} \cdot T$	-0.689 eV (b)
$\int_0^T C_{bound} dT'$	0.053 eV (a)	$\int_0^T C_{gas} dT'$	0.00918 eV (b)

Using equation S2 we can get the Gibbs integral energy from which we take the occupancy with the minimum energy as being the equilibrium for each potential and each facet. ΔZ_p is the difference in zero-point energy between the bound and gas-phase chlorine. ΔC is the change in heat capacity. $\Delta S^{int}(\theta)$ consists of the difference in entropy as well as the configurational entropy for a given coverage.⁶

$$\Delta G_{adsorp}^{int}(U) = N_{Cl} \left(\Delta E_{adsorp}^{avg}(U) + \Delta Z_p - T \Delta S^{int}(\theta) + \int_0^T \Delta C dT' \right) \quad (S2)$$

$$\Delta S^{int}(\theta) = S_{bound} - S_{gas} + S_{config}^{int}(\theta)$$

$$\Delta S_{config}^{int}(\theta) = -k_B \ln \left(\frac{\theta}{1-\theta} \right) - \frac{k_b}{\theta} \ln(1-\theta)$$

The Gibbs energy is plotted for two potentials in figure 4A and the concentration of the equilibrium as it is calculated here is plotted with the potential in figure 4C.

To get figure 4B, first we calculate the surface energy of the facet via equation S3. The bulk energy (E_{bulk}) is calculated with a system of 4 copper and with a k-points sampling of 10×10×10, the calculation is otherwise identical to previous. There exist a data base of the surface fractions and energies, their results have been calculated with a comparable methodology but without Van Der Waals correction.⁷

$$\gamma_{hkl} = \frac{E_{slab} - E_{bulk} N_{Cu}}{A_{surface}} \quad (S3)$$

Table S5: Copper nano-crystal in vacuum.

	Bulk energy structure of calculated model (eV)	Bulk energy pr atom (eV)
Cu	-303.434	-75.8585

Facet	Surface energy $\gamma_{hkl} \left(\frac{eV}{\text{\AA}^2} \right)$	Fraction %
(100)	0.086	25.2
(110)	0.091	10.6
(111)	0.079	59.2
(310)	0.093	5.0

Finally, the Gibbs energy can be added to the surface energies to get the surface tension for a given facet at equilibrium.

$$\gamma_{hkl}^{tension} = \gamma_{hkl} + \Delta G_{ad}^{int}(U) \quad (S4)$$

Structures

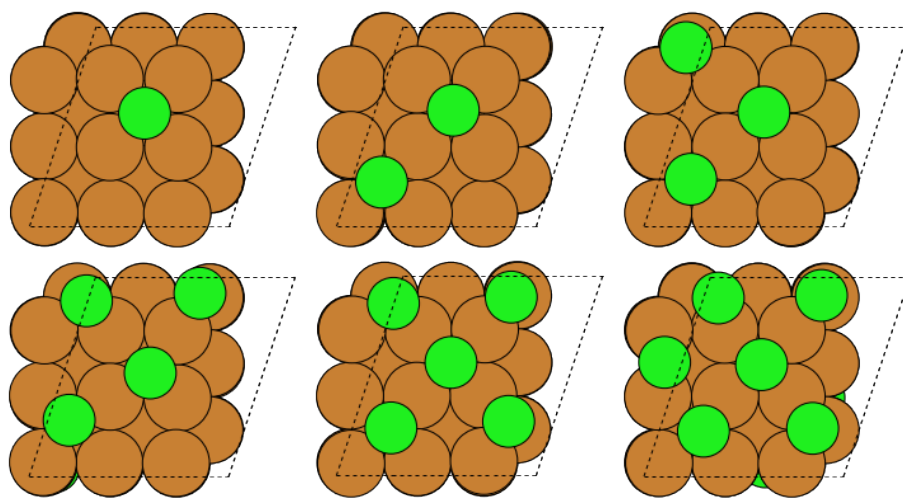


Figure S9: (100) Top from right to left: coverage at 0.016, 0.032 and $0.049 \text{ Cl}^* \text{ \AA}^{-2}$. Bottom from right to left: coverage at 0.065, 0.081 and $0.097 \text{ Cl}^* \text{ \AA}^{-2}$.

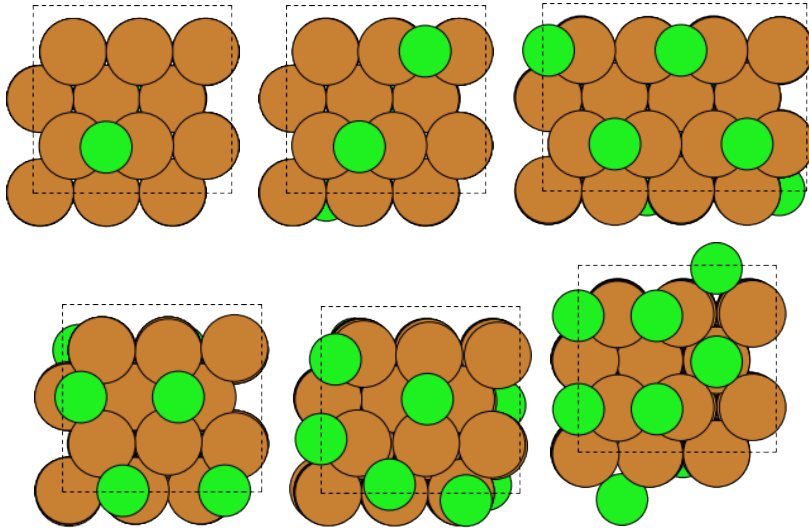


Figure S10: (110) Top from right to left: coverage at 0.017, 0.034 and $0.052 \text{ Cl}^* \text{ \AA}^{-2}$. Bottom from right to left: coverage at 0.069, 0.086 and $0.1 \text{ Cl}^* \text{ \AA}^{-2}$. The third image, upper right, have a bigger slab since the optimal packing pattern for this coverage (coverage = $0.052 \text{ Cl}^* \text{ \AA}^{-2}$) is irreducible to the smaller slab.

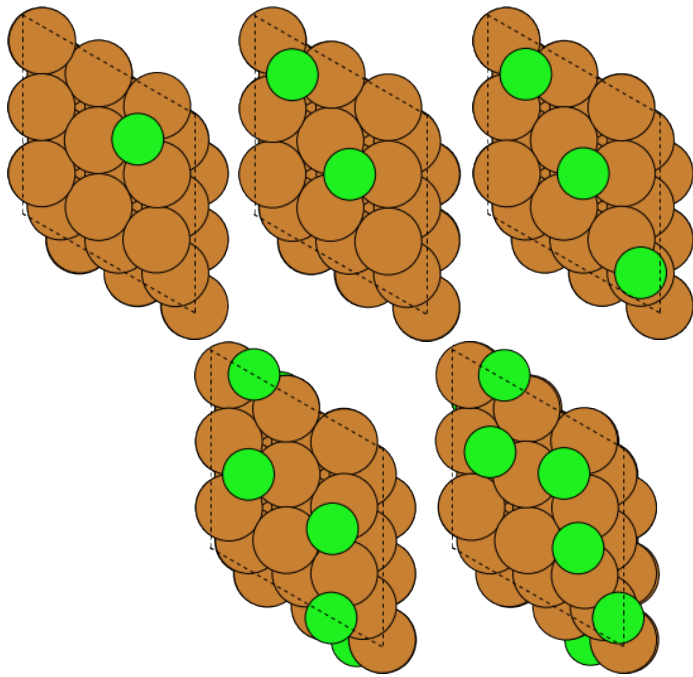


Figure S11: (111) Top from right to left: coverage at 0.019, 0.037 and 0.056 $Cl^* \text{ \AA}^{-2}$. Bottom from right to left: coverage at 0.075 and 0.094 $Cl^* \text{ \AA}^{-2}$.

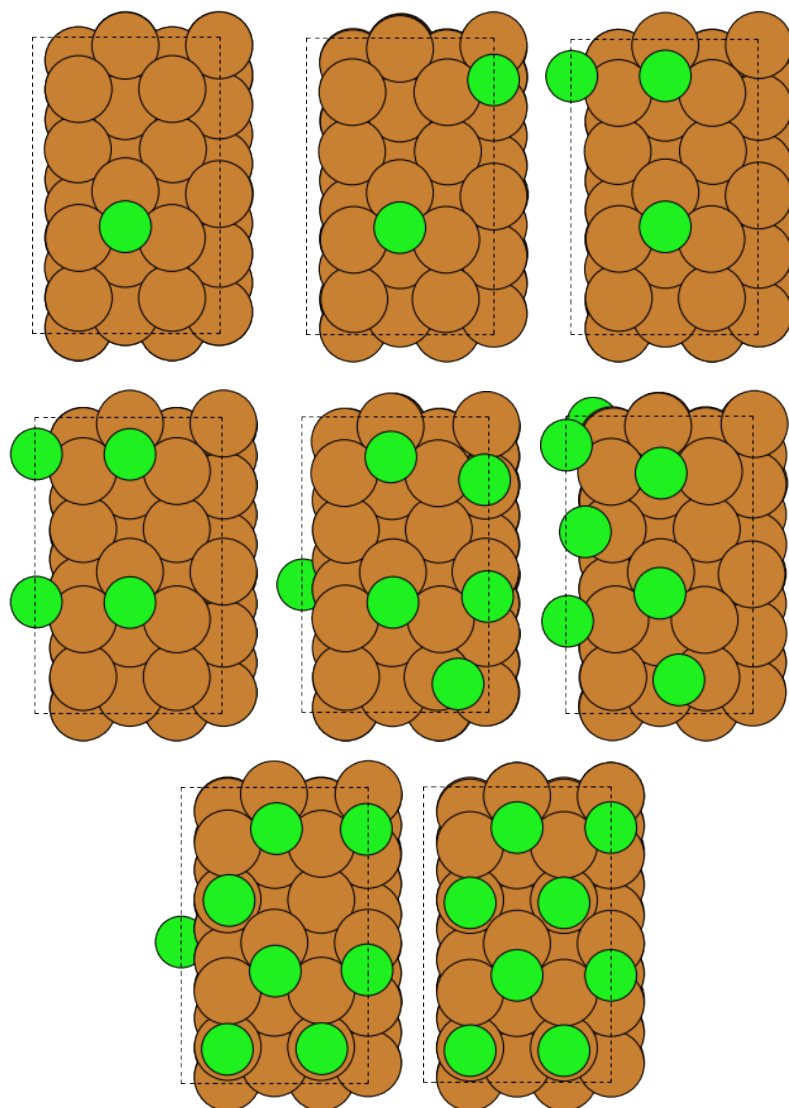


Figure S12: (310) Top from right to left: coverage at 0.012, 0.023 and 0.034 $Cl^* \text{Å}^{-2}$. Middle from right to left: coverage at 0.046, 0.058 and 0.069 $Cl^* \text{Å}^{-2}$. Bottom from right to left: coverage at 0.081 and 0.092 $Cl^* \text{Å}^{-2}$.

References

- 1 J. R. Rumble, D. M. Bickham and C. J. Powell, *Surf. Interface Anal.*, 1992, **19**, 241–246.
- 2 <https://janaf.nist.gov/>.
- 3 J. Enkovaara, C. Rostgaard, J. J. Mortensen, J. Chen, M. Dułak, L. Ferrighi, J. Gavnholt,

- C. Glinsvad, V. Haikola, H. A. Hansen, H. H. Kristoffersen, M. Kuisma, A. H. Larsen, L. Lehtovaara, M. Ljungberg, O. Lopez-Acevedo, P. G. Moses, J. Ojanen, T. Olsen, V. Petzold, N. A. Romero, J. Stausholm-Møller, M. Strange, G. A. Tritsarlis, M. Vanin, M. Walter, B. Hammer, H. Häkkinen, G. K. H. Madsen, R. M. Nieminen, J. K. Nørskov, M. Puska, T. T. Rantala, J. Schiøtz, K. S. Thygesen and K. W. Jacobsen, *J. Phys. Condens. Matter*, 2010, **22**.
- 4 S. R. Bahn and K. W. Jacobsen, *Comput. Sci. Eng.*, 2002, **4**, 56–66.
- 5 <https://nano.ku.dk/english/research/theoretical-electrocatalysis/katlabdb/copper-with-chloride>.
- 6 N. Garcia-Araez, V. Climent and J. Feliu, *J. Phys. Chem. C*, 2009, **113**, 19913–19925.
- 7 <http://crystalium.materialsvirtuallab.org/>.